Effect of the Breit interaction on inner-shell electron-impact excitation and subsequent radiative decay of highly charged berylliumlike ions

Z. W. Wu [1,*] M. M. Zhao,[2] C. Ren,[1] C. Z. Dong,[1] and J. Jiang[1]

[1]*Key Laboratory of Atomic and Molecular Physics & Functional Materials of Gansu Province, College of Physics and Electronic Engineering, Northwest Normal University, Lanzhou 730070, People's Republic of China*

[2]*College of Science, Gansu Agricultural University, Lanzhou 730070, People's Republic of China*

(Received 8 January 2020; accepted 14 January 2020; published 3 February 2020)

The inner-shell electron-impact excitation from the ground state to the $1s2s^22p_{1/2}\,J_f = 1$ excited state and the subsequent electric-dipole $1s2s^22p_{1/2}\,J_f = 1 \rightarrow 1s^22s^2\,J_i = 0$ radiative decay of berylliumlike ions with zero nuclear spin have been studied within the framework of the multiconfigurational Dirac-Fock method and the relativistic distorted-wave theory. Special attention has been paid to answering the question of how the Breit interaction affects such a two-step "excitation plus decay" process. To this end, we explore the effect of the Breit interaction on the second-order alignment parameter of the excited state and also the angular distribution of the emitted characteristic photons. It is found that, for low-Z berylliumlike ions such as Ne^{6+}, the Breit interaction hardly contributes to the alignment and the angular distribution even at high-impact electron energies. In contrast, the contribution from the Breit interaction for intermediate- and high-Z ions such as Mo^{38+}, W^{70+}, and U^{88+} is of the essence, and such a contribution becomes more and more significant with increasing atomic number and electron energy. To be more specific, the Breit interaction even changes qualitatively the relative population of the magnetic substates of the excited state as described by the alignment parameter and the angular emission pattern of the characteristic photons, for example, for W^{70+} and U^{88+} ions at the electron energies beyond 3.5 and 3.3 times the excitation thresholds, respectively.

DOI: 10.1103/PhysRevA.101.022701

I. INTRODUCTION

The significance of the Breit interaction among electrons in atoms or ions has been known for many decades since Gregory Breit proposed the theory of two-electron interactions beyond the well-known Coulomb interaction to study the fine-structure energy levels of helium atoms [1,2]. After undergoing many years of practice, such a theory was found fundamental to nuclear, atomic, molecular, and optical physics as well as to modern quantum electrodynamics [3]. Following this extraordinary masterwork, a great number of works have been carried out in atomic physics to explore the influence of the Breit interaction upon the fine- and hyperfine-structure energy levels [4–13], static and dynamic electric-dipole ($E1$) polarizabilities [14–17], magic wavelengths [17,18], parity-nonconserving transition amplitudes [19–21], radiative and nonradiative decays [22–28], electron-collision processes such as dielectronic recombination (DR) [29–31], electron-impact ionization [32–34], and electron-impact excitation (EIE) [35–37], photoexcitation and photoionization [38,39], as well as electron scattering of atoms or (highly charged) ions [40]. At present, the (full) Breit interaction or at least parts of it can be efficiently incorporated in most theoretical calculations of atomic structures and transition properties.

As well known, characteristic (x-ray) photons emitted from atoms or ions are regarded particularly as a very effective tool for exploring atomic structure and transition properties and, thus, have been applied to numerous case studies in atomic physics. Among those studies, much attention has been paid to angle- and polarization-resolved properties of the characteristic photons, such as the angular distribution and linear polarization [41,42]. When compared with total decay rates of the characteristic x-ray photons, these angle- and polarization-resolved physical observables are often found much more sensitive to various (weak) physical effects and interactions [43,44]. Owing to such a known sensitivity, the angular distribution and linear polarization of the characteristic photons have been used to investigate, for instance, the hyperfine interaction [43], the multipole mixing of radiation fields [44,45], and also the Breit interaction [46–53].

Motivated by the experimental work on "Evidence for strong Breit interaction in DR of highly charged heavy ions" performed by Nakamura *et al.* [29], Fritzsche and coworkers proposed two x-ray measurements on the angular distribution and linear polarization of the $E1$ radiation $1s2s^22p_{1/2}\,J_f = 1 \rightarrow 1s^22s^2\,J_i = 0$ of high-Z berylliumlike ions following the resonant electron capture into lithiumlike ions to reveal the dominance of the Breit interaction [46]. Such a proposal and the corresponding theoretical predictions were soon demonstrated experimentally by measuring the angular distribution of the $E1$ radiation from berylliumlike Au^{75+} ions with an electron-beam ion trap [47]. Since this seminal work [46], there has been continuous interest in further exploring the

*zhongwen.wu@nwnu.edu.cn

Breit-interaction effect by analyzing the angular distribution and linear polarization of characteristic photons [48–53]. For example, we studied the Breit-interaction effect upon the linear polarization of the same $E1$ radiations but following the EIE of berylliumlike ions by using the multiconfigurational Dirac-Fock (MCDF) method and the relativistic distorted-wave (RDW) theory [49]. It was found that such an effect depends significantly on the formation mechanism of the characteristic radiation, as discussed also in Ref. [54]. Jörg *et al.* [50] and Ren *et al.* [51] investigated experimentally and theoretically the effect of the Breit interaction upon the linear polarization of characteristic (x-ray) photons emitted from boronlike ions following their DR and EIE processes, respectively. In addition, atomic-number and state-selective influence of the Breit interaction upon the angular distribution of the emitted characteristic photons were also explored in DR experiments [52,53].

In this contribution, we investigate the inner-shell EIE of berylliumlike Ne^{6+}, Mo^{38+}, W^{70+}, and U^{88+} ions from their ground state to the excited state $1s2s^22p_{1/2}\,J_f = 1$ and also the subsequent $1s2s^22p_{1/2}\,J_f = 1 \rightarrow 1s^22s^2\,J_i = 0$ $E1$ radiative decay by using the MCDF method and the RDW theory. In particular, primary attention is paid to revealing the effect of the Breit interaction on such a two-step "excitation plus decay" process. Therefore, we explore the Breit-interaction effect on the alignment of the excited state, which reflects its magnetic-substate population in the inner-shell EIE process, and also on the angular distribution of the emitted $E1$ characteristic photons. By performing detailed theoretical calculations, we find that, for low-Z ions such as Ne^{6+}, the Breit interaction almost does not affect the alignment and the angular distribution even at high-impact electron energies. In contrast, however, for intermediate- and high-Z ions such as Mo^{38+}, W^{70+}, and U^{88+} the contribution of the Breit interaction is very important to both of them, and it becomes more and more pronounced with the increase of the atomic number and impact electron energy. More specifically, the Breit interaction even changes qualitatively the (relative) magnetic-substate population of the excited state as described by the second-order alignment parameter $\mathcal{A}_{20}$ and also the angular emission pattern of the characteristic photons, for example, for W^{70+} and U^{88+} ions at the impact electron energies beyond 3.5 and 3.3 times the excitation thresholds, respectively. It has been known that the presently considered $E1$ radiative decay predominates in the emission of characteristic photons over other (spin-forbidden) radiative photons of the excited state by more than four orders of magnitude [46]. Therefore, such a two-step "excitation plus decay" process of intermediate- and high-Z berylliumlike ions can be proposed for probing the Breit-interaction effect on relativistic electron-ion collisions. Currently, the proposed angle-resolved measurements of the characteristic x-ray photons are feasible with the use of the present-day experimental facilities, such as both the heavy-ion storage rings and electron-beam ion traps.

This paper is structured as follows: In the next section, a fully RDW formalism is presented to calculate the partial cross sections for the EIE to the individual magnetic substates of atoms or ions from their ground states. It is then applied to the two-step "excitation plus decay" process of berylliumlike ions to obtain the alignment parameter of the excited state $1s2s^22p_{1/2}\,J_f = 1$ and also the angular distribution of the emitted characteristic $1s2s^22p_{1/2}\,J_f = 1 \rightarrow 1s^22s^2\,J_i = 0$ photons. In Sec. III, we analyze the presently obtained results for the alignment parameter and the angular distribution and, in particular, reveal the effect of the Breit interaction on both of them. Finally, a brief conclusion of the present work is summarized in Sec. IV.

Atomic units ($m_e = 1$, $e = 1$, $\hbar = 1$) have been utilized throughout the paper unless stated otherwise.

II. THEORY AND COMPUTATION

A. Partial electron-impact-excitation cross sections

In the present work, a fully relativistic computer code REIE06 [55] is employed to calculate the required partial EIE cross sections, which was developed on the basis of the RDW theory. With this theory, if the incident impact electrons are assumed to be unpolarized and the quantization z axis is chosen along the propagation direction of the electrons, the partial EIE cross sections from the initial state $|\beta_i J_i M_i\rangle$ to the final state $|\beta_f J_f M_f\rangle$ of target ions can be expressed as [55,56]

$$\begin{aligned}\sigma(\beta_i J_i M_i \rightarrow \beta_f J_f M_f) = \frac{2\pi a_0^2}{k_i^2} \sum_{l_i j_i l_i' j_i' m_{s_i}} \sum_{l_f j_f m_f} \sum_{JJ'M} i^{(l_i - l_i')} [(2l_i+1)(2l_i'+1)]^{1/2} \exp\left[i\left(\delta_{\kappa_i(l_i j_i)} - \delta_{\kappa_i'(l_i' j_i')}\right)\right] \\ \times \langle l_i m_{l_i}, 1/2 m_{s_i} | j_i m_i\rangle \langle l_i' m_{l_i'}, 1/2 m_{s_i} | j_i' m_i\rangle \langle J_i M_i, j_i m_i | JM\rangle \langle J_i M_i, j_i' m_i | J'M\rangle \\ \times \langle J_f M_f, j_f m_f | JM\rangle \langle J_f M_f, j_f m_f | J'M\rangle R(\gamma_i, \gamma_f) R^*(\gamma_i', \gamma_f'). \end{aligned} \tag{1}$$

Here, the subscripts i and f signify, respectively, the initial and final states of the impact electrons and target ions. $1/2$, l_i, and j_i are the quantum numbers for the spin, orbital, and total angular momenta of the incident impact electrons, while the quantum numbers m_{s_i}, m_{l_i}, and m_i are, respectively, their z components. β_i denotes all additional quantum numbers required to specify particularly the initial state $|\beta_i J_i M_i\rangle$ of the target ions in addition to the total angular momentum J_i and its z component M_i. J and M denote the quantum numbers corresponding to the total angular momentum of the impact system "target ion plus impact electron" and its z component, respectively. $\gamma_i \equiv \varepsilon_i l_i j_i \beta_i J_i JM$, and $\gamma_f \equiv \varepsilon_f l_f j_f \beta_f J_f JM$. Moreover, other quantum numbers with the subscript f have similar implications but for the final state $|\beta_f J_f M_f\rangle$ or the outgoing electrons. The standard notation for the Clebsch-Gordan coefficients is used in Eq. (1). As the quantization z axis has been chosen along the direction of motion of the impact electrons, $m_{l_i} = m_{l_i'} = 0$ and, thus, $m_i = m_{s_i}$

owing to the properties of the Clebsch-Gordan coefficients. δ_{κ_i} denotes the phase factor of the impact electrons with the relativistic quantum number κ_i that is uniquely specified by the quantum numbers l_i and j_i. a_0 is the Bohr radius. k_i represents the relativistic wave number of the incident impact electrons, which is related to the corresponding kinetic energy ε_i by

$$k_i^2 = \varepsilon_i\left(1 + \frac{\alpha^2\varepsilon_i}{4}\right), \tag{2}$$

where α is the fine-structure constant.

The (reduced) EIE transition amplitudes $R(\gamma_i, \gamma_f)$ are independent of M and can be expressed as [55,56]

$$R(\gamma_i, \gamma_f) = \langle\Psi_{\gamma_f}| \sum_{p,\,q;\;p<q}^{\mathrm{N+1}} V_{ee} |\Psi_{\gamma_i}\rangle. \tag{3}$$

In this expression, Ψ_{γ_i} and Ψ_{γ_f} denote the antisymmetric $(N+1)$-electron wave functions for the initial and final states of the impact system, respectively. Moreover, the operator V_{ee} characterizes electron-electron interactions, which consist dominantly of the instantaneous Coulomb repulsion and the Breit interaction.

While the corresponding Coulomb operator takes the form of $V_{\mathrm{Coul}} = 1/r_{pq}$, the Breit operator is given by [57]

$$V_{\mathrm{Breit}} = -\frac{\boldsymbol{\alpha}_p \cdot \boldsymbol{\alpha}_q}{r_{pq}} \cos(\omega_{pq} r_{pq}) + (\boldsymbol{\alpha}_p \cdot \boldsymbol{\nabla}_p)(\boldsymbol{\alpha}_q \cdot \boldsymbol{\nabla}_q)\frac{\cos(\omega_{pq} r_{pq}) - 1}{\omega_{pq}^2 r_{pq}}, \tag{4}$$

which consists of the magnetic and retardation contributions (first and second term). In this expression, $\boldsymbol{\alpha}_p$ and $\boldsymbol{\alpha}_q$ denote the vectors of the Dirac matrices of electrons p and q, respectively. r_{pq} is the distance between the two electrons. ω_{pq} is the angular frequency of the exchanged virtual photon. $\boldsymbol{\nabla}_p$ represents the vector gradient operator as associated with the p electron.

B. Alignment parameter and angular distribution

With the partial EIE cross sections ready, as given by Eq. (1), the (relative) magnetic-substate population of the excited state $\beta_f J_f$ can be fully determined. Within the density-matrix theory [58,59], such a population is characterized most generally by so-called alignment parameters. For the particular EIE process from the ground state $1s^2 2s^2\, J_i = 0$ to the excited state $1s2s^2 2p_{1/2}\, J_f = 1$ of berylliumlike ions, the relative population of the excited state is given uniquely by an alignment parameter $\mathcal{A}_{20}$, which can be expressed in terms of the partial EIE cross sections as follows [46]:

$$\mathcal{A}_{20} = \sqrt{2}\frac{\sigma_{\pm1} - \sigma_0}{2\sigma_{\pm1} + \sigma_0}. \tag{5}$$

Here, σ_0 and $\sigma_{\pm1}$ represent the partial EIE cross sections corresponding to the excitations from the ground state to the magnetic substates $|M_f = 0\rangle$ and $|M_f = \pm1\rangle$ of the excited state $1s2s^2 2p_{1/2}\, J_f = 1$, respectively.

As well known, excited states of atoms or ions are unstable and may stabilize by the emission of one or several photons. Once the population of the excited states becomes known, the angle- and polarization-resolved emission properties of these atoms or ions would be fully determined. Therefore, the angular distribution and polarization of the emitted characteristic photons are closely related to the alignment parameters. For the subsequent $E1$ radiative decay $1s2s^2 2p_{1/2}\, J_f = 1 \to 1s^2 2s^2\, J_i = 0 + \gamma$ of berylliumlike ions following the EIE process, for instance, the angular distribution of the corresponding $E1$ photons γ can be expressed as [59–61]

$$\mathrm{W}(\theta) = 1 + \beta_2^{\mathrm{eff}} P_2(\cos\theta) \tag{6}$$

in the rest frame of the (projectile) ions. In this formula, β_2^{eff} represents the (effective) anisotropy parameter and is given by $\beta_2^{\mathrm{eff}} = \mathcal{A}_{20}/\sqrt{2}$. $P_2(\cos\theta)$ is the second-order Legendre polynomial with the polar angle θ of the emitted $E1$ photons that is determined by the propagation directions of the incident impact electrons and the emitted $E1$ photons. It should be noted that the angular distribution (6) has been normalized with respect to total intensity of the emitted $E1$ photons, i.e., $\mathrm{W}(90^\circ) = 1 - \beta_2^{\mathrm{eff}}/2$. In experiments, the angular distribution can be readily determined by recording the yields of the characteristic photons emitted along different polar angles at given azimuthal angles.

C. Evaluation of electron-impact-excitation transition amplitudes

As can be seen from Eqs. (1)–(6), any further analysis of the alignment of the excited state $1s2s^2 2p_{1/2}\, J_f = 1$ and the angular properties of the characteristic $E1$ photons should be traced back to the evaluation of the EIE transition amplitudes $R(\gamma_i, \gamma_f)$ as given by Eq. (3). However, since these transition amplitudes appear frequently in the studies of EIE properties of atoms or ions, such as, excitation strengths, cross sections, and rate coefficients [55,56,62], they can be acquired quite readily from different computer codes. Here, we follow our previous work [49,54] on the studies of x-ray polarizations and apply the RDW theory to evaluate the needed EIE amplitudes with the use of the MCDF wave functions.

In the MCDF method, an atomic-state wave function with specific parity P, total angular-momentum quantum number J, and its z component M is expressed in terms of the corresponding configuration-state wave functions (CSFs) with the same PJM [57,63],

$$\psi_\alpha(PJM) = \sum_{r=1}^{n_c} c_r(\alpha)|\phi_r(PJM)\rangle. \tag{7}$$

In this expression, n_c is the number of the CSFs used and the configuration mixing coefficients $\{c_r(\alpha)\}$ denote the representation of the atomic state ψ_α in the chosen basis $\{|\phi_r\rangle\}$. The CSFs are generated initially as an antisymmetrized product of a set of orthonormal orbitals and then optimized self-consistently in the basis of the Dirac-Coulomb (-Breit) Hamiltonian. This is followed by an incorporation of the quantum-electrodynamical effects into the representation $\{c_r(\alpha)\}$ of the atomic state ψ_α by diagonalizing the Dirac-Coulomb (-Breit) Hamiltonian matrix.

For the presently considered EIE from the ground state $1s^2 2s^2\, J_i = 0$ to the excited state $1s2s^2 2p_{1/2}\, J_f = 1$ and the subsequent radiative decay of berylliumlike ions, the configurations $1s^2 2s^2$, $1s2s^2 2p$, and $1s^2 2p^2$ are utilized to

TABLE I. EIE excitation energies (eV) from the ground state $1s^22s^2\,J_i = 0$ to the excited state $1s2s^22p_{1/2}\,J_f = 1$ of berylliumlike Ne^{6+}, Mo^{38+}, W^{70+}, and U^{88+} ions. NB and B stand for the results without and with the inclusion of the contribution from the Breit interaction, respectively.

Ions	Ne^{6+}	Mo^{38+}	W^{70+}	U^{88+}
NB	893.9	17842.4	59186.5	96522.7
B	893.6	17813.9	59014.0	96165.2

TABLE II. Comparison of the present alignment parameters $\mathcal{A}_{20}$ of the excited states $1s2s^22p_{1/2}\,J_f = 1$, $1s2s^22p_{3/2}\,J_f = 1$, and $1s2s^22p_{3/2}\,J_f = 2$ of berylliumlike Mo^{38+} ions with other available results [66] at the impact electron energy 20 keV.

Excited states	NB	NB [66]	B
$1s2s^22p_{1/2}\,J_f = 1$	−0.204	−0.199	−0.154
$1s2s^22p_{3/2}\,J_f = 1$	−0.655	−0.656	−0.648
$1s2s^22p_{3/2}\,J_f = 2$	−0.216	−0.217	−0.228

produce required wave functions and energy levels by means of GRASP92 [64]. Moreover, these wave functions and energy levels are employed further to evaluate the needed EIE transition amplitudes by using the RDW code REIE06 [55], in which the maximal partial waves are taken as $\kappa = \pm 50$ in order to ensure convergence. It should be noted that all calculations are performed twice respectively without and with the inclusion of the Breit interaction, from which the contribution of the Breit interaction can be extracted. It should be noted that the hyperfine interaction can cause depolarization of the excited states of atoms or ions with nonzero nuclear spin [65], such as the excited state $1s2s^22p_{1/2}\,J_f = 1$ considered in the present work. Nevertheless, in the present work we consider just the case of the EIE and subsequent radiative decay of berylliumlike ions with zero nuclear spin and, accordingly, the relevant theory and computation are presented just for such a case.

III. RESULTS AND DISCUSSION

Before moving forward, it should be clear that the results labeled by "NB" as given below are calculated with the inclusion of only the Coulomb interaction in the corresponding matrix elements, while those labeled by "B" are obtained by taking both the Coulomb and Breit interactions into account. In Table I, we list the presently calculated excitation energies (in units of eV) for the inner-shell EIE from the ground state $1s^22s^2\,J_i = 0$ to the excited state $1s2s^22p_{1/2}\,J_f = 1$ of berylliumlike Ne^{6+}, Mo^{38+}, W^{70+}, and U^{88+} ions. To examine the contribution of the Breit interaction to the excitation energies, results are given for both the cases NB and B, respectively. As can be seen from the table, the excitation energies without the inclusion of the Breit interaction are overestimated by 0.3, 28.5, 172.5, and 357.5 eV for these highly charged berylliumlike ions, respectively, when compared with those results labeled by B. That is to say, the contribution from the Breit interaction to the EIE excitation energies reaches 0.03%, 0.16%, 0.29%, and 0.37%, respectively. It is obvious that the effect of the Breit interaction on the excitation energies becomes more significant for higher-Z ions.

To illustrate the accuracy and reliability of the present calculations, we list the alignment parameters $\mathcal{A}_{20}$ of the excited states $1s2s^22p_{1/2}\,J_f = 1$, $1s2s^22p_{3/2}\,J_f = 1$, and $1s2s^22p_{3/2}\,J_f = 2$ of berylliumlike Mo^{38+} ions at the impact electron energy 20 keV in Table II, together with other available results for comparison. The referenced alignment parameters in the column labeled by "NB" [66] are calculated with the use of the corresponding partial EIE cross sections as given in Ref. [66]. By comparing the presently obtained alignment parameters $\mathcal{A}_{20}$ with the available ones from Ref. [66] in the case of NB, we find that the agreement between the two theoretical results is excellent not only for the excited state $1s2s^22p_{1/2}\,J_f = 1$ considered presently but also for the states $1s2s^22p_{3/2}\,J_f = 1$ and $1s2s^22p_{3/2}\,J_f = 2$. The maximal (relative) discrepancy is found to be just 2.5%. Such an excellent agreement ensures the validity of the present calculations on the energy levels and wave functions as well as the corresponding partial EIE cross sections for the berylliumlike ions considered.

In Fig. 1, we present the alignment parameters $\mathcal{A}_{20}$ of the excited state $1s2s^22p_{1/2}\,J_f = 1$ following the inner-shell EIE of berylliumlike Ne^{6+}, Mo^{38+}, W^{70+}, and U^{88+} ions, as functions of the impact electron energy in threshold units. Results are given for both the NB and B cases. It should be noted that the coordinate scale utilized for Ne^{6+} ions is

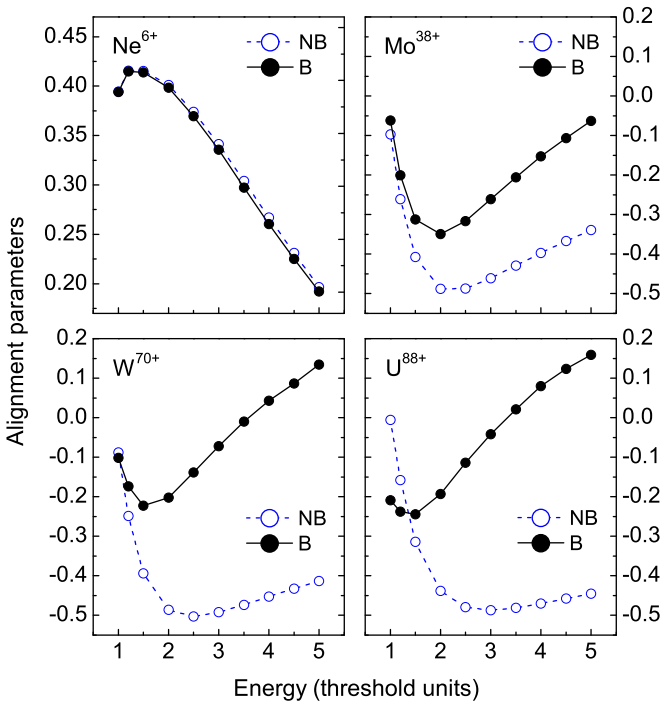

FIG. 1. Alignment parameters $\mathcal{A}_{20}$ of the $1s2s^22p_{1/2}\,J_f = 1$ excited state following the EIE of berylliumlike Ne^{6+} (top-left panel), Mo^{38+} (top right), W^{70+} (bottom left), and U^{88+} (bottom right) ions, as functions of the impact electron energy (in threshold units). NB (blue dashed lines with open circles) and B (black solid lines with solid circles) stand for the results without and with the inclusion of the contribution from the Breit interaction, respectively.

different from those for the other three ions. As seen from the figure, while the Breit interaction hardly contributes to the alignment parameters $\mathcal{A}_{20}$ for low-Z ions such as Ne^{6+} even at high impact electron energies, the contribution of the Breit interaction to $\mathcal{A}_{20}$ is essential for intermediate- and high-Z ions and, in fact, it becomes more significant for higher-Z ions at higher energies. For instance, the absolute contribution of the Breit interaction to $\mathcal{A}_{20}$ changes from 0.28 for Mo^{38+} to 0.60 for U^{88+} at the electron energy of five times their respective excitation thresholds, i.e., an increase by two times more. Also, take W^{70+} ions for example, such an absolute contribution increases significantly from 0.07 to 0.55 with increasing electron energy from 1.2 to 5 times the excitation threshold. Nevertheless, the present theoretical calculations show that the alignment parameter $\mathcal{A}_{20}$ evolves smoothly from the Ne^{6+} type to the Mo^{38+} one with increasing ionic charge state. Moreover, due to the effect of the Breit interaction, $\mathcal{A}_{20}$ changes the sign from negative to positive at the energies of 3.5 and 3.3 times the excitation thresholds for W^{70+} and U^{88+} ions, respectively. Such a change of the sign indicates that at higher electron energies the magnetic substates $|M_f = \pm 1\rangle$ become predominantly populated over the substate $|M_f = 0\rangle$ in the EIE process of (intermediate- and high-Z) berylliumlike ions, as can be understood from Eq. (5).

It is found that the alignment parameters $\mathcal{A}_{20}$ are very sensitive to the impact electron energy for all of the ions, although the overall dependence of $\mathcal{A}_{20}$ on the energy for low-Z ions such as Ne^{6+} ions is remarkably different from the situation for intermediate- and high-Z ions. Nevertheless, the particular behavior of $\mathcal{A}_{20}$ is still different in the regions of low- and high-impact energies for both the cases without and with the inclusion of the Breit interaction. To be specific, at the impact electron energies lower than two times the excitation thresholds, the alignment parameters $\mathcal{A}_{20}$ corresponding to Mo^{38+}, W^{70+}, and U^{88+} ions for the case NB are more strongly dependent on the energy than those for the case B, while the situation is just the opposite in the high-energy region. Moreover, the two curves of $\mathcal{A}_{20}$ for U^{88+} ions are found to be crossed at the electron energy of 1.4 times the thresholds, which indicates that, at this particular energy, the Breit interaction does not contribute to the (relative) population on the magnetic substates $|M_f = 0, \pm 1\rangle$ of the excited state $1s2s^22p_{1/2}\,J_f = 1$ in the associated EIE process of U^{88+} ions. Actually, such a cross occurs first for berylliumlike ions with $Z \approx 70$ at their excitation thresholds, and the position of intersection moves toward higher electron energies with increasing atomic number Z.

Apart from the effect of the Breit interaction upon the inner-shell EIE process of berylliumlike ions, as characterized by the alignment parameters $\mathcal{A}_{20}$, such an effect on the subsequent radiative decay of the $1s2s^22p_{1/2}\,J_f = 1$ excited state is also investigated by exploring the angular distribution of the characteristic (x-ray) photons emitted from the $1s2s^22p_{1/2}\,J_f = 1 \rightarrow 1s^22s^2\,J_i = 0$ $E1$ radiative decay. For example, Fig. 2 displays the angular distribution for the four berylliumlike ions at the impact electron energy of four times their respective excitation thresholds. Again, results are given for both the cases NB and B. As expected from the analysis on the alignment parameters $\mathcal{A}_{20}$, for low-Z Ne^{6+} ions the Breit interaction does not influence the angular distribution of the

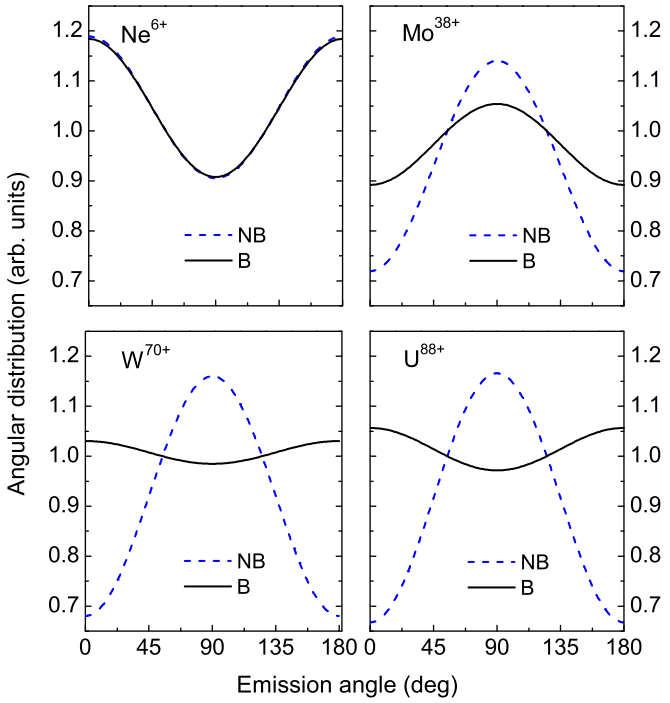

FIG. 2. Angular distribution of the characteristic (x-ray) photons emitted from the $1s2s^22p_{1/2}\,J_f = 1 \rightarrow 1s^22s^2\,J_i = 0$ $E1$ radiative decay following the EIE of berylliumlike Ne^{6+} (top-left panel), Mo^{38+} (top right), W^{70+} (bottom left), and U^{88+} (bottom right) ions at the impact electron energy of four times their respective excitation thresholds. Results are presented for both the NB (blue dashed lines) and B (black solid lines) cases. The calculations are performed for the projectile frame, in which the impact electrons are in motion.

characteristic photons, and the photons are dominantly emitted along the impact electron-beam axis z under $\theta = 0^\circ$ and 180° for both cases. With respect to intermediate- and high-Z ions, however, the situation becomes fairly different. While the characteristic photons are dominantly emitted perpendicular to the beam axis z for the angular distribution obtained from the Dirac-Coulomb theory (i.e., for the case NB), a quantitative and even qualitative change in the photon emission pattern occurs when the contribution from the Breit interaction is further taken into account. To be more specific, at the given impact electron energy of four times the thresholds, the angular distribution of the $1s2s^22p_{1/2}\,J_f = 1 \rightarrow 1s^22s^2\,J_i = 0$ $E1$ photons is predicted to become first isotropic for $Z \approx 70$ from perpendicularly dominant photon emissions and, then, more and more pronounced along the beam z axis with increasing atomic number Z of berylliumlike ions. As can be seen from the figure, for berylliumlike W^{70+} and U^{88+} ions, the photon emissions along the electron-beam axis are clearly favored. Such presently obtained characteristics of the Breit-interaction effect on the photon angular distribution are quite similar to the conclusions summarized for the angular distribution of the same $E1$ photon emissions but following the resonant electron capture into initially lithiumlike ions [46].

Besides the Breit-interaction effect on the angular distribution of the characteristic $E1$ photons emitted from different ions at given impact electron energies, moreover, we also explore the energy dependence of such an effect. Here,

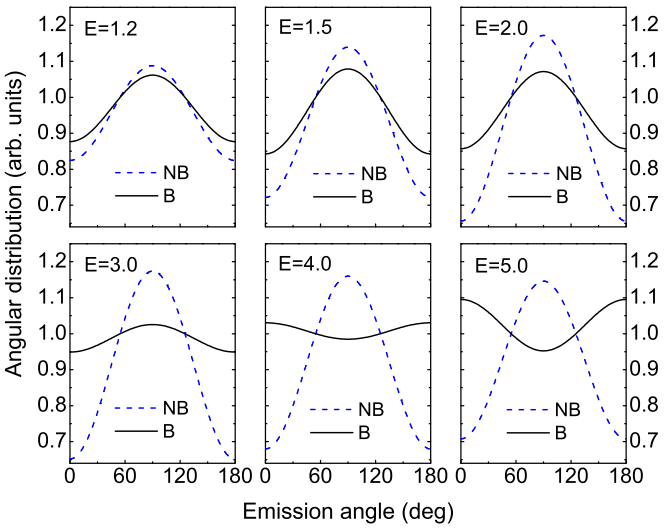

FIG. 3. Angular distribution of the characteristic (x-ray) photons emitted from the $1s2s^22p_{1/2}\,J_f = 1 \rightarrow 1s^22s^2\,J_i = 0$ $E1$ radiative decay following the EIE of berylliumlike W^{70+} ions at different impact electron energies in the threshold units: 1.2 (top left), 1.5 (top middle), 2.0 (top right), 3.0 (bottom left), 4.0 (bottom middle), and 5.0 (bottom right). The calculations are performed in the projectile frame.

we take W^{70+} ions for example and plot the corresponding angular distribution at various impact energies, as shown in Fig. 3. It is found that, for all of the electron energies considered, the angular distribution without the Breit interaction included dominates in the direction perpendicular to the electron-beam axis (i.e., $\theta = 90^\circ$), and it is almost independent of the impact energy, especially at energy regions higher than 1.5 times the excitation threshold. By contrast, the inclusion of the contribution from the Breit interaction makes the properties of the angular distribution very different, which alters even the emission pattern of the characteristic photons at high-impact electron energies. With the increase of the impact electron energy, the angular distribution of the $1s2s^22p_{1/2}\,J_f = 1 \rightarrow 1s^22s^2\,J_i = 0$ photons is found to become first isotropic at the energy of about 3.5 times the excitation threshold and, then, behave more and more pronounced along the electron-beam axis.

Based on the detailed analysis of the Breit-interaction effect upon the alignment parameters $\mathcal{A}_{20}$ of the excited state $1s2s^22p_{1/2}\,J_f = 1$ and the angular distribution of the emitted characteristic photons, it has been found that the EIE and subsequent radiative decay of intermediate- and high-Z berylliumlike ions are significantly influenced by the contributions from the Breit interaction. Furthermore, it has been known that the presently considered $E1$ radiative decay of the excited state $1s2s^22p_{1/2}\,J_f = 1$ to the ground state $1s^22s^2\,J_i = 0$ predominates in the x-ray photon emissions over other spin-forbidden transitions of the excited state by at least four orders of magnitude [46]. Therefore, the inner-shell EIE and the subsequent $E1$ decay of intermediate- and high-Z berylliumlike ions can be proposed for probing the details of the Breit-interaction effect on relativistic electron-ion collisions. The proposed measurements are feasible with the use of the present-day experimental facilities, such as both the heavy-ion storage rings and electron-beam ion traps.

IV. CONCLUSION

To summarize, the inner-shell EIE from the ground state to the $1s2s^22p_{1/2}\,J_f = 1$ excited state and the subsequent $E1$ radiative decay of berylliumlike Ne^{6+}, Mo^{38+}, W^{70+}, and U^{88+} ions have been investigated within the framework of the MCDF method and the RDW theory. Special attention has been paid to answering the question of how the Breit interaction could affect such a two-step "excitation plus decay" process. To do so, we explore the effect of the Breit interaction on the alignment of the excited state $1s2s^22p_{1/2}\,J_f = 1$ and also the angular distribution of the emitted characteristic $E1$ photons. It is found that, for low-Z ions, the Breit interaction hardly contributes to the alignment of the excited state even at high-impact electron energies, while for intermediate- and high-Z ions the contribution of the Breit interaction is of the essence and it becomes more important for higher-Z ions at higher electron energies. For instance, for W^{70+} and U^{88+} ions the Breit interaction even changes the sign of the alignment parameters $\mathcal{A}_{20}$ from negative to positive at high electron energies, which indicates that the magnetic substates $|M_f = \pm 1\rangle$ of the $1s2s^22p_{1/2}\,J_f = 1$ excited state become predominantly populated over the substate $|M_f = 0\rangle$ in the energetic EIE of these ions.

Moreover, with respect to the subsequent radiative decay, the characteristic photons are dominantly emitted perpendicular to the electron-beam axis for intermediate- and high-Z ions if the Breit interaction is not included. Such a photon emission pattern is nearly independent of the atomic number and the electron energy especially in the high-energy region. However, the situation becomes very different when the contribution from the Breit interaction is taken into account and, to be specific, a quantitative and even qualitative change is caused in the emission pattern of the characteristic photons. At the given electron energy of four times the excitation thresholds, for instance, the angular distribution of the emitted $E1$ photons becomes first isotropic for $Z \approx 70$ from perpendicularly dominant emissions and, then, more and more pronounced along the electron-beam z axis with increasing atomic number of berylliumlike ions. Besides, the Breit interaction also makes the angular distribution more dependent on the impact electron energy. As the increase of the electron energy, take W^{70+} ions for example, the Breit-interaction effect makes the angular distribution of the $1s2s^22p_{1/2}\,J_f = 1 \rightarrow 1s^22s^2\,J_i = 0$ photons become first isotropic at the energy of about 3.5 times the threshold from perpendicularly dominant emissions, and then behave more pronounced along the beam axis.

Admittedly, the (relative) population of the magnetic substates of atoms or highly charged ions as described by the alignment and the angle-resolved emissions of characteristic (x-ray) photons have been found much more sensitive to various (weak) physical effects and interactions when compared with total transition rates or strengths [43,44]. Therefore, such an exploration could help reveal more detailed information of the Breit-interaction effect on relativistic electron-ion collisions.

ACKNOWLEDGMENTS

This work is supported by the National Key Research and Development Program of China (2017YFA0402300). Z.W.W. acknowledges the National Natural Science Foundation of China (NSFC) under Grant No. 11804280, the Scientific Research Funding of the Higher Education Institutions of Gansu Province of China under Grant No. 2018A-002, and the Major Project of the Research Ability Promotion Program for Young Scholars of Northwest Normal University of China under Grant No. NWNU-LKQN2019-5. The NSFC under Grants No. 11864036, No. 11774292, and No. 11874051 is also acknowledged.

[1] G. Breit, Phys. Rev. **34**, 553 (1929).
[2] G. Breit, Phys. Rev. **36**, 383 (1930).
[3] M. Hull, *Biographical Memoirs* (The National Academy Press, Washington, DC, 1998), Vol. 74.
[4] R. Si, X. L. Guo, T. Brage, C. Y. Chen, R. Hutton, and C. F. Fischer, Phys. Rev. A **98**, 012504 (2018).
[5] T. H. Dinh and V. A. Dzuba, Phys. Rev. A **94**, 052501 (2016).
[6] A. V. Malyshev, A. V. Volotka, D. A. Glazov, I. I. Tupitsyn, V. M. Shabaev, and G. Plunien, Phys. Rev. A **90**, 062517 (2014).
[7] M. S. Safronova, V. A. Dzuba, V. V. Flambaum, U. I. Safronova, S. G. Porsev, and M. G. Kozlov, Phys. Rev. A **90**, 052509 (2014).
[8] V. A. Yerokhin and A. Surzhykov, Phys. Rev. A **86**, 042507 (2012).
[9] P. Imgram, K. König, J. Krämer, T. Ratajczyk, R. A. Müller, A. Surzhykov, and W. Nörtershäuser, Phys. Rev. A **99**, 012511 (2019).
[10] N. Aourir, M. Nemouchi, M. Godefroid, and P. Jönsson, Phys. Rev. A **97**, 032506 (2018).
[11] M. Lochmann, R. Jöhren, C. Geppert, Z. Andelkovic, D. Anielski, B. Botermann, M. Bussmann, A. Dax, N. Frömmgen, M. Hammen, V. Hannen, T. Kühl, Y. A. Litvinov, R. López-Coto, T. Stöhlker, R. C. Thompson, J. Vollbrecht, A. Volotka, C. Weinheimer, W. Wen, E. Will, D. Winters, R. Sánchez, and W. Nörtershäuser, Phys. Rev. A **90**, 030501(R) (2014).
[12] O. P. Sushkov, Phys. Rev. A **63**, 042504 (2001).
[13] W. R. Johnson, K. T. Cheng, and D. R. Plante, Phys. Rev. A **55**, 2728 (1997).
[14] Y.-H. Zhang, L.-Y. Tang, X.-Z. Zhang, and T.-Y. Shi, Phys. Rev. A **93**, 052516 (2016).
[15] S. Chattopadhyay, B. K. Mani, and D. Angom, Phys. Rev. A **91**, 052504 (2015).
[16] W. R. Johnson and K. T. Cheng, Phys. Rev. A **53**, 1375 (1996).
[17] Y.-B. Tang, B.-Q. Lou, and T.-Y. Shi, Phys. Rev. A **96**, 022513 (2017).
[18] F.-F. Wu, S.-J. Yang, Y.-H. Zhang, J.-Y. Zhang, H.-X. Qiao, T.-Y. Shi, and L.-Y. Tang, Phys. Rev. A **98**, 040501(R) (2018).
[19] V. A. Dzuba, C. Harabati, W. R. Johnson, and M. S. Safronova, Phys. Rev. A **63**, 044103 (2001).
[20] A. Derevianko, Phys. Rev. Lett. **85**, 1618 (2000).
[21] A. Derevianko, Phys. Rev. A **65**, 012106 (2001).
[22] M. Bilal, A. V. Volotka, R. Beerwerth, and S. Fritzsche, Phys. Rev. A **97**, 052506 (2018).
[23] C. Mendoza and M. A. Bautista, Phys. Rev. Lett. **118**, 163002 (2017).
[24] E. A. Konovalova and M. G. Kozlov, Phys. Rev. A **92**, 042508 (2015).
[25] S. Kasthurirangan, J. K. Saha, A. N. Agnihotri, S. Bhattacharyya, D. Misra, A. Kumar, P. K. Mukherjee, J. P. Santos, A. M. Costa, P. Indelicato, *et al.*, Phys. Rev. Lett. **111**, 243201 (2013).
[26] L. Natarajan, Phys. Rev. A **92**, 012507 (2015).
[27] V. I. Korobov, Phys. Rev. A **67**, 062501 (2003).
[28] M. H. Chen and B. Crasemann, Phys. Rev. A **35**, 4579 (1987).
[29] N. Nakamura, A. P. Kavanagh, H. Watanabe, H. A. Sakaue, Y. Li, D. Kato, F. J. Currell, and S. Ohtani, Phys. Rev. Lett. **100**, 073203 (2008).
[30] D. Bernhardt, C. Brandau, Z. Harman, C. Kozhuharov, A. Müller, W. Scheid, S. Schippers, E. W. Schmidt, D. Yu, A. N. Artemyev, I. I. Tupitsyn, S. Böhm, F. Bosch, F. J. Currell, B. Franzke, A. Gumberidze, J. Jacobi, P. H. Mokler, F. Nolden, U. Spillman, Z. Stachura, M. Steck, and T. Stöhlker, Phys. Rev. A **83**, 020701(R) (2011).
[31] K. N. Lyashchenko and O. Y. Andreev, Phys. Rev. A **91**, 012511 (2015).
[32] O. Y. Andreev, E. A. Mistonova, and A. B. Voitkiv, Phys. Rev. Lett. **112**, 103202 (2014).
[33] M. K. Inal, H. L. Zhang, D. H. Sampson, and C. J. Fontes, Phys. Rev. A **65**, 032727 (2002).
[34] C. J. Fontes, D. H. Sampson, and H. L. Zhang, Phys. Rev. A **59**, 1329 (1999).
[35] A. Gumberidze, D. B. Thorn, A. Surzhykov, C. J. Fontes, B. Najjari, A. Voitkiv, S. Fritzsche, D. Banaś, H. F. Beyer, W. Chen *et al.*, Phys. Rev. A **99**, 032706 (2019).
[36] A. Gumberidze, D. B. Thorn, C. J. Fontes, B. Najjari, H. L. Zhang, A. Surzhykov, A. Voitkiv, S. Fritzsche, D. Banaś, H. Beyer *et al.*, Phys. Rev. Lett. **110**, 213201 (2013).
[37] C. J. Fontes, H. L. Zhang, and D. H. Sampson, Phys. Rev. A **59**, 295 (1999).
[38] A. M. Sossah, H.-L. Zhou, and S. T. Manson, Phys. Rev. A **86**, 023403 (2012).
[39] S. N. Nahar, M. Montenegro, W. Eissner, and A. K. Pradhan, Phys. Rev. A **82**, 065401 (2010).
[40] C. J. Bostock, D. V. Fursa, and I. Bray, Phys. Rev. A **80**, 052708 (2009).
[41] N. Kabachnik, S. Fritzsche, A. Grum-Grzhimailo, M. Meyer, and K. Ueda, Phys. Rep. **451**, 155 (2007).
[42] N. Nakamura, J. Phys. B: At., Mol. Opt. Phys. **49**, 212001 (2016).
[43] Z. W. Wu, A. Surzhykov, and S. Fritzsche, Phys. Rev. A **89**, 022513 (2014).
[44] A. Surzhykov, S. Fritzsche, A. Gumberidze, and T. Stöhlker, Phys. Rev. Lett. **88**, 153001 (2002).
[45] G. Weber, H. Bräuning, A. Surzhykov, C. Brandau, S. Fritzsche, S. Geyer, S. Hagmann, S. Hess, C. Kozhuharov, R. Märtin *et al.*, Phys. Rev. Lett. **105**, 243002 (2010).
[46] S. Fritzsche, A. Surzhykov, and T. Stöhlker, Phys. Rev. Lett. **103**, 113001 (2009).

[47] Z. Hu, X. Han, Y. Li, D. Kato, X. Tong, and N. Nakamura, Phys. Rev. Lett. **108**, 073002 (2012).
[48] C. Shah, H. Jörg, S. Bernitt, S. Dobrodey, R. Steinbrügge, C. Beilmann, P. Amaro, Z. Hu, S. Weber, S. Fritzsche *et al.*, Phys. Rev. A **92**, 042702 (2015).
[49] Z. W. Wu, J. Jiang, and C. Z. Dong, Phys. Rev. A **84**, 032713 (2011).
[50] H. Jörg, Z. Hu, H. Bekker, M. A. Blessenohl, D. Hollain, S. Fritzsche, A. Surzhykov, J. R. Crespo López-Urrutia, and S. Tashenov, Phys. Rev. A **91**, 042705 (2015).
[51] C. Ren, Z. W. Wu, J. Jiang, L. Y. Xie, D. H. Zhang, and C. Z. Dong, Phys. Rev. A **98**, 012711 (2018).
[52] Z. Hu, Y. Li, X. Han, D. Kato, X. Tong, H. Watanabe, and N. Nakamura, Phys. Rev. A **90**, 062702 (2014).
[53] P. Amaro, C. Shah, R. Steinbrügge, C. Beilmann, S. Bernitt, J. R. C. López-Urrutia, and S. Tashenov, Phys. Rev. A **95**, 022712 (2017).
[54] Z. W. Wu, C. Z. Dong, and J. Jiang, Phys. Rev. A **86**, 022712 (2012).
[55] J. Jiang, C. Z. Dong, L. Y. Xie, and J. G. Wang, Phys. Rev. A **78**, 022709 (2008).
[56] H. L. Zhang, D. H. Sampson, and R. E. H. Clark, Phys. Rev. A **41**, 198 (1990).
[57] I. P. Grant, *Relativistic Quantum Theory of Atoms and Molecules: Theory and Computation* (Springer-Verlag, New York, 2007).
[58] K. Blum, *Density Matrix Theory and Applications*, 3rd ed. (Springer-Verlag, Berlin, Heidelberg, 2012).
[59] V. V. Balashov, A. N. Grum-Grzhimailo, and N. M. Kabachnik, *Polarization and Correlation Phenomena in Atomic Collisions* (Kluwer Academic, New York, 2000).
[60] Z. W. Wu, N. M. Kabachnik, A. Surzhykov, C. Z. Dong, and S. Fritzsche, Phys. Rev. A **90**, 052515 (2014).
[61] Z. W. Wu, A. V. Volotka, A. Surzhykov, and S. Fritzsche, Phys. Rev. A **96**, 012503 (2017).
[62] S. Mahmood, S. Ali, I. Orban, S. Tashenov, E. Lindroth, and R. Schuch, Astrophys. J. **754**, 86 (2012).
[63] J. P. Desclaux, Comput. Phys. Commun. **9**, 31 (1975).
[64] F. Parpia, C. Fischer, and I. Grant, Comput. Phys. Commun. **94**, 249 (1996).
[65] U. Fano and J. H. Macek, Rev. Mod. Phys. **45**, 553 (1973).
[66] M. H. Chen and K. J. Reed, Phys. Rev. A **50**, 2279 (1994).